CHEMISTRY
A EUROPEAN JOURNAL

DOI: 10.1002/chem.200800804

Reactivity of Transition Metal–Phosphorus Triple Bonds towards Triply Bonded [{CpMo(CO)$_2$}$_2$]: Formation of Heteronuclear Cluster Compounds

Manfred Scheer,*[a] Daniel Himmel,[b] Christian Kuntz,[a] Shuzhong Zhan,[c] and Eva Leiner[a]

Dedicated to Professor Wolfgang A. Herrmann on the occasion of his 60th birthday

Abstract: Thermolysis of [Cp*P{W(CO)$_5$}$_2$] (**1**) in the presence of [{CpMo(CO)$_2$}$_2$] leads to the novel complexes [{(CO)$_2$Cp*W}-{CpMo(CO)$_2$}(μ,η^2:η^1:η^1-P$_2${W(CO)$_5$}$_2$)] (**6**; Cp = η^5-C$_5$H$_5$, Cp* = η^5-C$_5$Me$_5$), [{(μ-O)(CpMoWCp*)W(CO)$_4$}{μ$_3$-PW(CO)$_5$}$_2$] (**7**), [{CpMo(CO)$_2$}$_2$-{Cp*W(CO)$_2$}{μ$_3$-PW(CO)$_5$}] (**8**) and [{CpMo(CO)$_2$}$_2${Cp*W(CO)$_2$}(μ$_3$-P)] (**9**). The structural framework of the main products **8** and **9** can be described as a tetrahedral Mo$_2$WP unit that is formed by a cyclisation reaction of [{CpMo(CO)$_2$}$_2$] with an [Cp*(CO)$_2$W≡P→W(CO)$_5$] intermediate containing a W–P triple bond and subsequent metal–metal and metal–phosphorus bond formation. Photolysis of **1** in the presence of [{CpMo(CO)$_2$}$_2$] gives **8**, **9** and phosphinidene complex [(μ$_3$-PW(CO)$_5$){CpMo(CO)$_2$W(CO)$_5$}] (**10**), in which the P atom is in a nearly trigonal-planar coordination environment formed by one {CpMo(CO)$_2$} and two {W(CO)$_5$} units. Comprehensive structural and spectroscopic data are given for the products. The reaction pathways are discussed for both activation procedures, and DFT calculations reveal the structures with minimum energy along the stepwise Cp* migration process under formation of the intermediate [Cp*(CO)$_2$W≡P→W(CO)$_5$].

Keywords: cluster compounds · molybdenum · phosphorus · reactive intermediates · tungsten

Introduction

Compounds containing triple bonds between metals and main group elements are a fascinating field in contemporary chemistry.[1] Particularly for Group 15 elements, a number of stable compounds having terminal pnicogenido ligands of the general formula [L$_n$M≡E] were synthesised by Cummins et al. (E = P; L$_n$M = (RR′N)$_3$Mo, (R$_2$N)$_3$Nb$^-$),[2] Schrock et al. (E = P, As; L$_n$M = N(CH$_2$CH$_2$NSiMe$_3$)$_3$W)[3] and us (E = P, As, Sb; ML$_n$ = N(CH$_2$CH$_2$NSiMe$_3$)$_3$W).[4] Furthermore, we prepared stable asymmetrically bridged compounds of the type [(RO)$_3$W≡P→W(CO)$_5$] (R = *t*Bu, 2,4-Me$_2$C$_6$H$_3$)[5] with a triple bond between tungsten and phosphorus. On the other hand, strategies are known for generating triply bonded compounds as highly reactive intermediates.[6] Recently, Ruiz et al. reported on an approach to intermediates of formula [Mo$_2$Cp$_2$(μ-κ^1:κ^1,η^4-PR)(CO)$_3$].[7] In contrast, some time ago we reported that thermolysis of phosphinidene complex [Cp*P{W(CO)$_5$}$_2$] (**1**)[8] leads to formation of a highly reactive intermediate with a metal–phosphorus triple bond.[9] Its generation is based on the Cp* migration from the σ-bound phosphorus atom to the tungsten atom in an η^5 coordination mode (Scheme 1).

Thus, thermolysis of **1** leads via CO elimination to intermediate **B** containing a P–W triple bond. In the absence of any reactive species, intermediate **B** dimerises to form the tetrahedral P$_2$W$_2$ complex **2**. As a side reaction, C–H bond

[a] Prof. Dr. M. Scheer, Dr. C. Kuntz, Dr. E. Leiner
Institut für Anorganische Chemie der Universität Regensburg
93040 Regensburg (Germany)
Fax: (+49) 941-943-4439
E-mail: manfred.scheer@chemie.uni-regensburg.de

[b] Dr. D. Himmel
Present address:
Institut für Anorganische und Analytische Chemie
der Albert-Ludwigs Universität Freiburg
79104 Freiburg in Breisgau (Germany)

[c] Dr. S. Zhan
Present address:
Department of the Applied Chemistry
South China University of Technology
Guangzhou 510640 (China)

Supporting information for this article is available on the WWW under http://dx.doi.org/10.1002/chem.200800804.

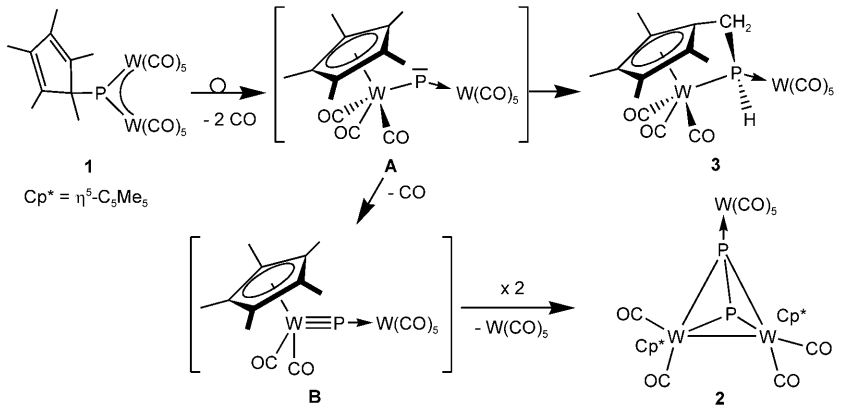

Scheme 1. Proposed reaction pathway for thermolysis of **1**.

activation of the possible intermediate **A** yields the phosphane complex **3**.

Photolysis of **1** leads to complex **4**,[10] which can be regarded to form from two reactive intermediates (Scheme 2): triply bonded intermediate **B**, formed by Cp* migration (Scheme 1), and a second intermediate **C** created by elimination of the Cp* moiety.

The existence of a reactive intermediate **B** is confirmed when the thermolysis is carried out in the presence of different trapping compounds. Thus, with alkynes novel metal-containing heterocycles and cage compounds are generated.[11] With phosphaalkynes novel phosphorus-rich cage compounds are obtained and, additionally, an unusual opening of the Cp* ligand is observed to form an unprecedented 1,2-diphosphacyclooctatetraene ligand.[12] The results obtained so far open up broad perspectives for the use of these intermediates in different trapping reactions. Herein we report on trapping reactions of intermediates **B** and **C**, generated in situ, with transition metal complexes containing multiple bonds. Density functional calculations give insight into the Cp* migration process to form intermediates **A** and **B** as well as energetic and structural aspects of the formation of all postulated intermediates along the reaction pathway. In addition, the electronic structure of intermediate **C** is presented.

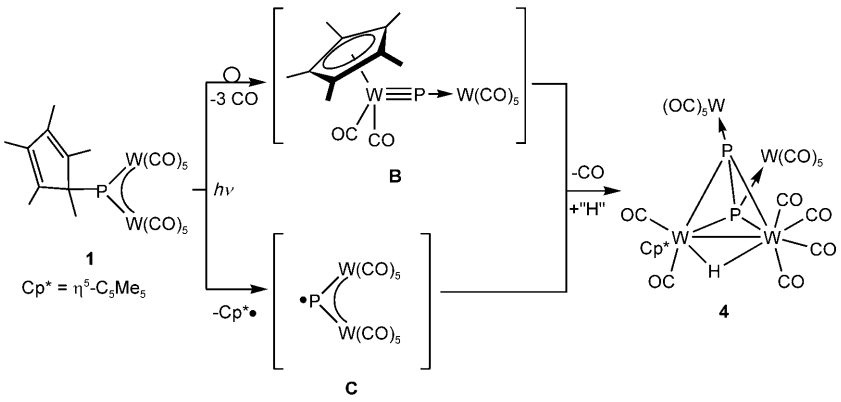

Scheme 2. Proposed reaction pathway for photolysis of **1**.

Results and Discussion

Thermolysis of [Cp*P{W(CO)$_5$}$_2$] (1) in the presence of [{CpMo(CO)$_2$}$_2$]: Thermolysis of a solution of **1** in toluene in the presence of [{CpMo(CO)$_2$}$_2$] for two hours results in the formation of compounds **3**, **5**, **6** and **7**[13] as minor products as well as complexes **8** and **9** as the main products [Eq. (1)]. Complexes **5**–**9** were obtained after column-chromatographic workup. The quantities of the isolated products are in accordance with the ^{31}P NMR spectrum of the crude reaction mixture. The only additional product that was observed ($\delta = 77.9$ ppm (s), $J_{W,P} = 136$ Hz) could not be obtained after chromatographic workup.

Photolysis of [Cp*P{W(CO)$_5$}$_2$] (1) in the presence of [{CpMo(CO)$_2$}$_2$]: Photolysis of **1** in toluene at room temperature in the presence of [{CpMo(CO)$_2$}$_2$] results in a colour change from blue to brown after two hours, which indicates complete transformation of **1**. After column-chromatographic workup, complexes **5**, **8** and main product **9** were isolated [Eq. (2)], that is, the tetrahedral Mo_2WP complexes are, like in the thermolysis reaction, the preferred products. In addition to the thermolysis products, in the photolysis reaction phosphinidene complex [(μ_3-PW(CO)$_5$)-{CpMo(CO)$_2$W(CO)$_5$}] (**10**) is formed in 30% yield. In accordance with the ^{31}P NMR spectrum of the crude reaction mixture, there is no further indication of different reaction products in detectable amounts, and thus all reaction products are isolated in appropriate quantities. The occurrence of Mo dimer **5** under thermal and photolytic conditions indicates the CO-accepting function of the triply bonded starting material.

Spectroscopic properties: Compounds **6**–**10** are sparingly soluble in *n*-hexane and readily soluble in CH_2Cl_2 and toluene. The IR spectra of all compounds reveal absorptions for terminal CO ligands. In the mass spectra the corresponding molecular-ion peak is observed in all cases, with the exception of **7** and **8**, for which the heaviest fragments detected correspond to loss of a {W(CO)$_5$} and a Cp moiety, respectively.

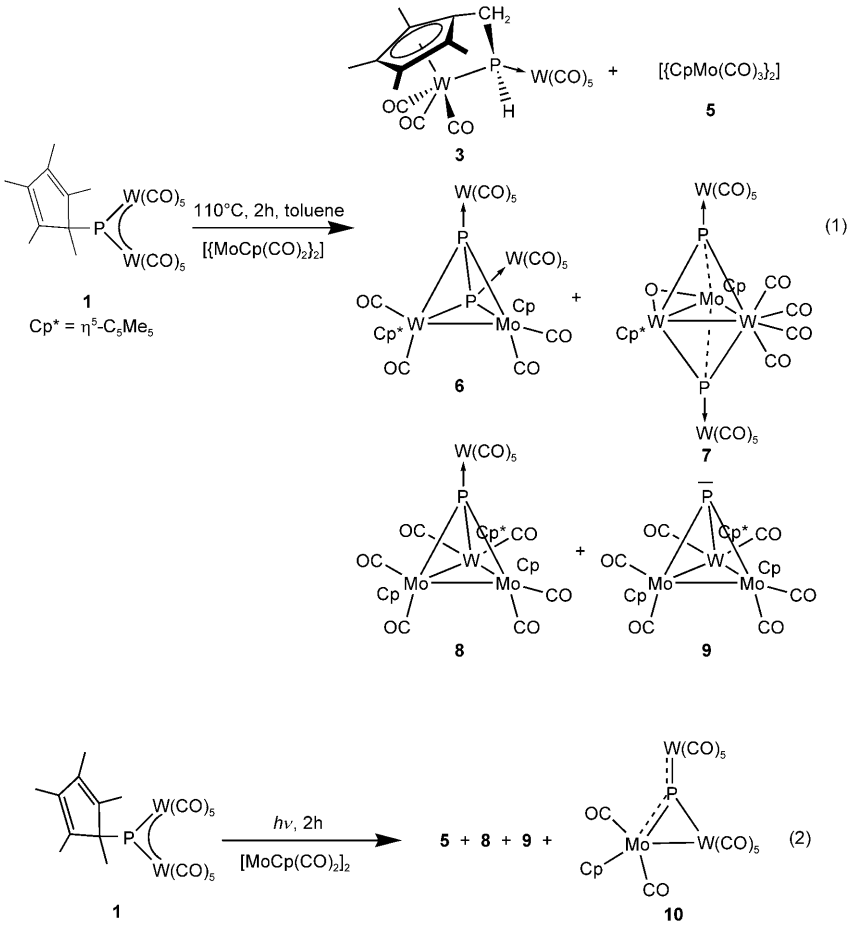

In the $^{31}P\{^1H\}$ NMR spectrum of **6**, observation of an AX spin system at $\delta = -188.1$ and -301.2 ppm ($^1J_{P,P} = 412.6$ Hz) indicates non-equivalent P atoms. This magnetic non-equivalence probably results from the different orientations of P atoms P1 and P2 with respect to the W and Mo atoms, which bear Cp* and Cp ligands. The $^{31}P\{^1H\}$ NMR spectrum of **7** reveals a singlet at $\delta = 279.3$ ppm with three pairs of tungsten satellites having $^{183}W,^{31}P$ coupling constants of 200, 100 and 39 Hz. Whereas the magnitude of the first coupling constant is consistent with bonding of a phosphorus atom to a terminal $\{W(CO)_5\}$ moiety, the other two coupling constants indicate the lower s character in the bonds to the tungsten atoms in the $\{Cp^*W\}$ and the $\{W(CO)_4\}$ fragments. Complex **9** displays one singlet in the $^{31}P\{^1H\}$ NMR spectrum at $\delta = 500$ ppm, which is significantly shifted downfield in comparison with that for **8** ($\delta = 153.8$ ppm). The singlet of **8** has two pairs of tungsten satellites with $^1J_{W,P} = 196$ and 76 Hz. The first coupling constant is consistent with bonding of a phosphorus atom to the terminal $\{W(CO)_5\}$ moiety; the latter indicates the low s character of the bonding to the $\{Cp^*W(CO)_2\}$ fragment and is in accordance with the $^1J_{W,P}$ value of 40.7 Hz found in **9**. For **10** the $^{31}P\{^1H\}$ NMR spectrum reveals a singlet at $\delta = 882.5$ ppm with two pairs of tungsten satellites having coupling constants of 191 and 55 Hz and is comparable to those found for other phosphinidene complexes,[14] for example, $[\{\mu_3\text{-}PCr(CO)_5\}\{CpCr(CO)_2\text{-}W(CO)_5\}]$ ($\delta = 945$ ppm).[15]

Crystal structure analysis: Crystallographic data are listed in Table 1. The molecular structure of the red crystalline compound $[(CO)_2Cp^*WCpMo(CO)_2(\mu,\eta^2\text{-}P_2\{W(CO)_5\}_2)]$ (**6**) is described as a slightly distorted P_2MoW tetrahedron, containing a $\{Cp^*(CO)_2W\}$ and a $\{Cp(CO)_2Mo\}$ unit (Figure 1). Both of the phosphorus atoms coordinate to the $\{W(CO)_5\}$ groups. Comparison of the P–W and P–Mo bond lengths in **6** show that each of the P atoms is more closely bound to one of the metal atoms of the tetrahedral P_2MoW unit. Thus, the P1–W1 and P1–Mo bond lengths are 2.521(4) and 2.429(3) Å, respectively, as opposed to the P2–W1 and P2–Mo bond lengths of 2.421(4) and 2.551(4) Å, respectively. The P–P bond length of **6** (2.099(6) Å) is comparable to those of similar M_2P_2 tetrahedral complexes, for example, $[Cp^*_2(CO)_4W_2(\mu,\eta^2\text{-}P_2)\{W(CO)_5\}]$ (**2**; 2.092(4) Å),[9] but is significantly shorter than the average single-bond length in β-P_4 of −185 °C (2.190 to 2.212 Å).[16]

Complex $[\{(\mu\text{-}O)(CpMoWCp^*)W(CO)_4\}(\mu_3\text{-}P\{W(CO)_5\})_2]$ (**7**) crystallises as brown sticks in the triclinic space group $P\bar{1}$ with one molecule of benzene in the unit cell. The molecular structure of **7** can be described as a W_2Mo triangle consisting of a $\{W(CO)_4\}$, a $\{Cp^*W\}$ and a $\{CpMo\}$ unit capped by two P atoms (Figure 2). The two μ_3-P ligands are coordinated to $\{W(CO)_5\}$ moieties, and the W1–Mo bond is bridged by an O ligand.[13] The W1–Mo bond (2.514(1) Å) is significantly shorter than the W2–Mo bond (2.989(1) Å) of the MoW_2 triangular unit. The short W1–Mo distance, which suggests a multiple bond is present, is comparable to that of 2.562(1) Å in $[MoW_2\{\mu\text{-}\sigma,\sigma':\eta^4\text{-}C(Ph)C(Ph)C(C_6H_4Me\text{-}4)\}(CO)_6Cp_2]$,[17] which has a Mo–W triple bond. On the other hand, it could also be caused by the bridging O atom, since the Mo–W bond length is comparable with that in $[NMe_4][Mo_2W(\mu_3\text{-}O)(\mu\text{-}O)_3(NCS)_9]$ (2.517(5)–2.527(5) Å).[18] The W2–Mo bond length is in the usual range of Mo–W single-bond lengths, for example, in $[CpW(CO)_2Mo(CO)_5(\mu\text{-}PPh_2)]$ (3.205(2) Å).[19] The P–W bond lengths (2.385(3), 2.433(3), 2.477(3), 2.489(3) Å) and P–Mo distances (2.456(3), 2.391(3) Å) of the W_2Mo triangle are as expected for such compounds.[20]

Table 1. Crystallographic data for **6**–**10**.

	6	**7**·0.5 C_6D_6	**8**·0.5 C_7H_8	**9**	**10**
formula	$C_{29}H_{20}MoO_{14}P_2W_3$	$C_{29}H_{20}MoO_{15}P_2W_4$·0.5 C_6H_6	$C_{31}H_{25}Mo_2O_{11}PW_2$·0.5 C_7H_8	$C_{26}H_{25}Mo_2O_6PW$	$C_{17}H_5MoO_{12}PW_2$
M_r	1301.88	1540.78	1210.13	840.16	895.82
crystal size [mm]	0.30×0.20×0.06	0.20×0.08×0.02	0.25×0.15×0.01	0.30×0.30×0.10	0.14×0.10×0.03
T [K]	200(1)	203(1)	200(1)	200(1)	203(2)
space group	$P2_1/c$	$\bar{P}1$	$P2_1/c$	$Pca2_1$	$P2_1/n$
crystal system	monoclinic	triclinic	monoclinic	orthorhombic	monoclinic
a [Å]	17.595(4)	10.205(2)	21.175(4)	14.637(3)	7.4224(15)
b [Å]	12.018(2)	11.687(2)	12.162(2)	14.274(3)	18.269(4)
c [Å]	17.235(3)	18.237(4)	43.135(9)	12.119(2)	17.366(4)
α [°]	90	87.59(3)	90	90.00	90
β [°]	105.04(3)	74.80(3)	104.21(3)	90.00	101.13(3)
γ [°]	90	66.64(3)	90	90.00	90
V [Å^3]	3519.9(12)	1922.2(7)	10769(4)	2532.1(9)	2310.5(8)
Z	4	2	12	4	4
ρ_{calcd} [g cm^{-3}]	2.457	2.662	2.239	2.204	2.575
μ [mm^{-1}]	6.659	7.703	7.174	5.611	7.419
radiation (λ [Å])	$Ag_{K\alpha}$ (0.56087)	$Ag_{K\alpha}$ (0.56087)	$Mo_{K\alpha}$ (0.71073)	$Mo_{K\alpha}$ (0.71073)	$Ag_{K\alpha}$ (0.56087)
diffractometer	STOE IPDS	STOE IPDS	STOE IPDS	STOE IPDS	STOE IPDS
2Θ range [°]	1.77–20.00	1.70–20.00	1.95–25.99	1.99–26.43	1.89–21.00
index range	$-21\le h\le 17$, $-14\le k\le 14$, $-21\le l\le 21$	$-11\le h\le 12$, $-14\le k\le 14$, $-22\le l\le 18$	$-25\le h\le 25$, $-14\le k\le 13$, $-52\le l\le 53$	$-12\le h\le 17$, $-18\le k\le 14$, $-14\le l\le 14$	$-9\le h\le 8$, $-23\le k\le 18$, $-22\le l\le 22$
data/restrains/parameters	6429/0/447	6788/0/492	20152/0/1391	4431/1/330	4850/0/298
independent reflections with $I>2\sigma(I)$	6429 ($R_{int}=0.0878$)	6788 ($R_{int}=0.0639$)	20152 ($R_{int}=0.0483$)	4431 ($R_{int}=0.0275$)	4850 ($R_{int}=0.0599$)
GOF on F^2	1.071	1.073	1.020	1.088	1.033
R_1,[a] wR_2[b] [$I>2\sigma(I)$]	0.0578, 0.1416	0.0490, 0.1285	0.0511, 0.1354	0.0343, 0.0926	0.0443, 0.1015
R_1,[a] wR_2[b] (all data)	0.0830, 0.1546	0.0613, 0.1365	0.0675, 0.1443	0.0345, 0.0927	0.0662, 0.1121
largest diff. peak and hole [e Å^{-3}]	1.545, −2.565	1.777, −2.195	7.850, −3.164	0.851, −1.196	1.727, −1.910

[a] $R_1=\Sigma||F_o|-|F_c||/\Sigma|F_o|$, $wR_2=[\Sigma w(F_o^2-F_c^2)^2/\Sigma w(F_o^2)^2]^{1/2}$.

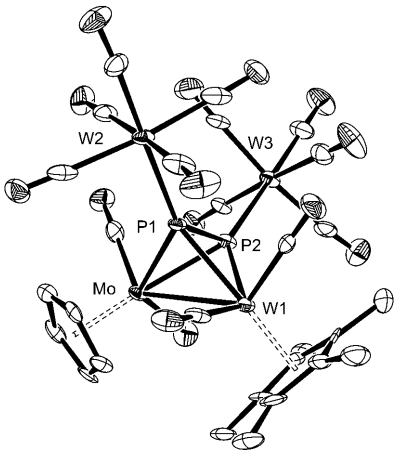

Figure 1. Molecular structure of **6** in the crystal (30% probability ellipsoids; hydrogen atoms omitted for clarity). Selected distances [Å] and angles [°]: P1–W1 2.521(4), P2–W1 2.421(4), P1–Mo 2.429(3), P2–Mo 2.551(4), W1–Mo 3.082(1), P1–W2 2.506(4), P2–W3 2.532(4), P1–P2 2.099(6); Mo-P1-W1 76.98(10), Mo-P2-W1 76.54(11), Mo-W1-P1 50.17(8), Mo-W1-P2 53.63(9), P1-W1-P2 50.22(14), P1-Mo-P2 49.78(14), W1-P2-P1 67.35(15).

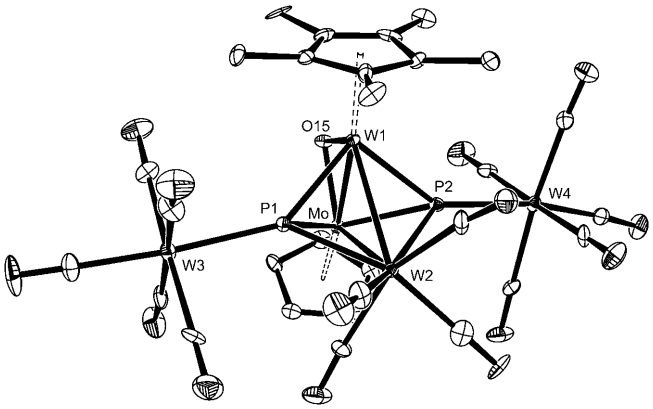

Figure 2. Molecular structure of **7** in the crystal (30% probability ellipsoids; hydrogen atoms omitted for clarity). Selected distances [Å] and angles [°]: P1–Mo 2.456(3), P2–Mo 2.391(3), P1–W1 2.385(3), P1–W2 2.489(3), P1–W3 2.516(3), P2–W1 2.433(3), P2–W2 2.477(3), P2–W4 2.515(3), W1–W2 3.027(1), W1–Mo 2.514(1), W2–Mo 2.989(1), W1–O15 1.895(8), Mo–O15 1.945(9); W1-Mo-W2 66.09(4), Mo-W2-W1 49.39(3), W2-W1-Mo 64.52(3).

The green crystals of [{$CpMo(CO)_2$}$_2${$Cp^*W(CO)_2$}{μ_3-$PW(CO)_5$}] (**8**) crystallise in the monoclinic space group $P2_1/c$ with 0.5 molecules of toluene per molecular unit in the crystal lattice and three independent molecules in the asymmetric unit with similar structural features. In the following, the structural pattern of molecule **A** is discussed (Figure 3).

The central framework of [{$CpMo(CO)_2$}$_2${$Cp^*W(CO)_2$}-{μ_3-$PW(CO)_5$}] (**8**) consists of a nearly ideal Mo_2W triangle (59.79(3)–60.27(2)°) of a {$Cp^*W(CO)_2$} unit and two {$CpMo(CO)_2$} units, capped by a P atom. The μ_3-P ligand co-

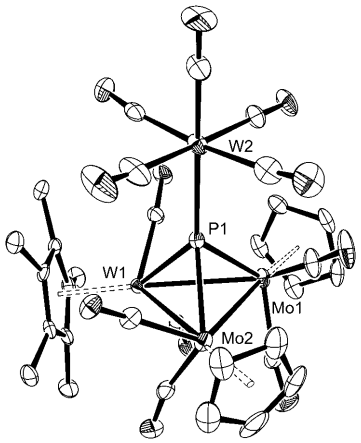

Figure 3. Molecular structure of **8** in the crystal (molecule **A**; 30% probability ellipsoids; hydrogen atoms omitted for clarity). Selected distances [Å] and angles [°]: P1–Mo1 2.486(3), P1–Mo2 2.466(3), P1–W1 2.466(2), P1–W2 2.571(3), Mo1–Mo2 3.070(1), Mo1–W1 3.080(1), Mo2–W 3.065(1); Mo1-W1-Mo2 59.93(3), W1-Mo1-Mo2 59.79(3), W1-Mo2-Mo1 60.27(2).

ordinates to a terminal $W(CO)_5$ group. The P1–W2 bond length (2.571(3) Å) is slightly elongated in comparison to other coordinative P–W bonds, for example, in $[Ph_3P\rightarrow W(CO)_5]$ (2.545(1) Å),[21] but is in the same range as in the W_2P_2 tetrahedrane complex $[\{Cp^*(CO)_6W_2\}(\mu\text{-}H)(\mu,\eta^1{:}\eta^1{:}\eta^1\text{-}P_2)\{W(CO)_5\}_2]$ (2.547(4) and 2.519(4) Å).[10] The P–Mo distances (2.486(3) und 2.466(3) Å) are in the usual range found for PMo tetrahedral cluster compounds.

Like complex **8** the structure of the brown crystalline compound **9** can also be described as a Mo_2W trinuclear cluster, capped by a P atom (Figure 4). In contrast to **8**, in **9** the P atom does not coordinate to a $\{W(CO)_5\}$ group. The Mo–Mo and Mo–W bond lengths (3.079(1), 3.109(1), 3.048(2) Å) and angles in the Mo_2W triangle of **9** (59.00(2)–60.99(2)°) are in the usual ranges for such complexes and similar to those observed for **8**.

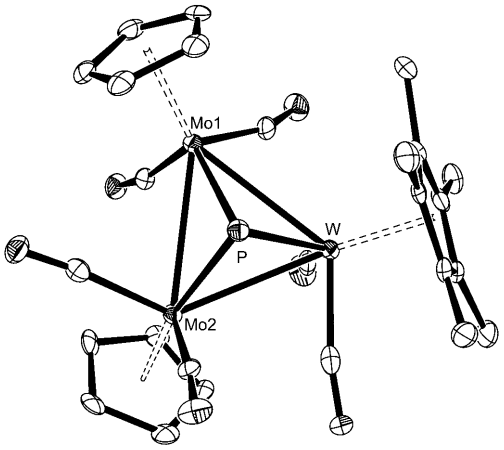

Figure 4. Molecular structure of **9** in the crystal (30% probability ellipsoids; hydrogen atoms omitted for clarity). Selected distances [Å] and angles [°]: P–Mo1 2.481(2), P–Mo2 2.400(2), P–W 2.411(2), Mo1–Mo2 3.079(1), Mo1–W 3.109(1), Mo2–W; W-Mo1-Mo2 59.00(2), Mo1-W-Mo2 60.01(2), Mo1-Mo2-W 60.99(2).

Phosphinidene complex **10** crystallises in the form of black platelets in the monoclinic space group $P2_1/n$. Its molecular structure is depicted in Figure 5. The central atom in the molecular structure of **10** is the nearly trigonal-planar P atom coordinated by a $\{CpMo(CO)_2\}$ and two $\{W(CO)_5\}$ units. The exocyclic P–W distance of 2.444(2) Å is about 0.09 Å shorter than the endocyclic P–W distance (2.536(3) Å). This indicates that the endocyclic P–W bond in the three-membered MoPW ring has the weakest π bonding. Thus, the P–W1 and P–Mo (2.296(2) Å) bonds are significantly shorter than usual single bonds.[20,22] These observations correspond with similar distances found, for example, in the phosphinidene complexes $[(\mu_3\text{-}P)\{Cr(CO)_5\}\text{-}\{CpW(CO)_2Cr(CO)_5\}]$ ($P\text{–}Cr_{exo}$ 2.305(5), $P\text{–}Cr_{endo}$ 2.428(5) Å).[23] The Mo–W2 bond length (3.168(1) Å) corresponds to an Mo–W single bond, as found in complexes like $[MoW_2(\mu_3\text{-}As)Cp_3(CO)_6]$ (3.097(2) and 3.124(2) Å)[24] as well as in **8** (3.080(1), 3.065(1) Å) and **9** (3.109(1), 3.0475(8) Å).

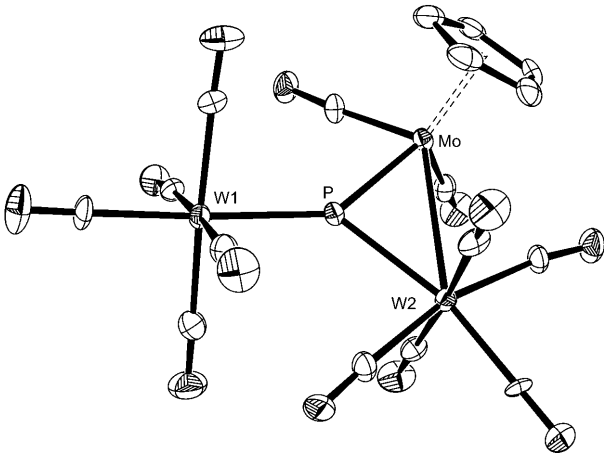

Figure 5. Molecular structure of **10** in the crystal (30% probability ellipsoids; hydrogen atoms omitted for clarity). Selected distances [Å] and angles [°]: P–Mo 2.296(2), P–W1 2.444(2), P–W2 2.536(3), Mo–W2 3.168(1); W1-P-Mo 142.49(12), W2-P-Mo 81.78(7), W1-P-W2 135.20(11), W1-Mo-W2-P 2.93(0).

Theoretical calculations: Due to their high reactivity intermediates **A** and **B** cannot be isolated. Therefore, DFT calculations were carried out to gain better insight into their structures and reactivity patterns. The optimised structures of **A** and **B** are depicted in Figure 6.

In both compounds the P atoms are sterically less shielded and thus highly reactive. For comparison of the W–P bond lengths in the calculated triply bonded intermediate **B**, the structurally characterised and stable compound $[(t\text{BuO})_3W{\equiv}P\rightarrow W(CO)_5]$ (**D**),[5b] which also contains a W–P triple bond and a coordinative P–W bond, was optimised at the same level of theory. A C_s-symmetric structure $\mathbf{D}_{calcd}$ was

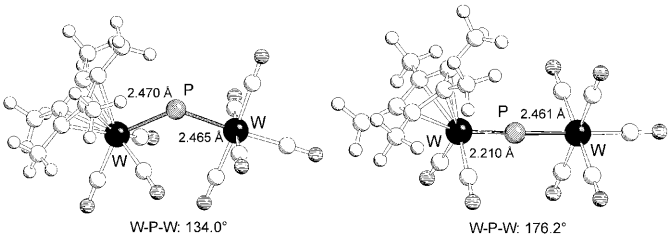

Figure 6. Calculated structures of intermediates **A** (left) and **B** (right) at the BP86/SV(P) level of theory.

obtained in which both W–P distances agree well (although slightly elongated) with the experimental data of the X-ray structure of **D**. The optimisation results show that in **B** 1) the coordinative bond length to the $\{W(CO)_5\}$ moiety (2.461 Å) is significantly shorter than in $\mathbf{D}_{calcd}$ (2.540 Å), which may be a result of better π backbonding from the $W(CO)_5$ moiety to the phosphido tungsten fragment. In contrast, 2) the calculated W–P triple bond in **B** (2.210 Å) is elongated compared to alkoxo compound $\mathbf{D}_{calcd}$ (2.158 Å). The latter fact also corresponds with the situation in $[(N_3N)W{\equiv}P{\rightarrow}GaCl_3]$ (2.168(4) Å;[25] $N_3N = N(CH_2CH_2NSiMe_3)_3$), whereas in *trans*-$[\{(N_3N)W{\equiv}P\}_2W(CO)_4]$ (2.202(2) and 2.460(2) Å)[4a] the distances are in agreement with the calculated values for **B**. Both tendencies are in line with the representative behaviour of phosphinidene complexes.[26] Complex **B** has π-acceptor ligands at the W atom and a more electrophilic P atom, while in **D** the triply bonded tungsten atom, which is surrounded by σ- and π-donor ligands, is in its highest oxidation state and the P atom is more nucleophilic with a stronger multiple bond.

The calculated structure of intermediate **C** (Figure 7) reveals shorter W–P distances than calculated for the precursor compound $[Cp^*P\{W(CO)_5\}_2]$ (**1**) and a larger W-P-W bond angle. This indicates steric relaxation of the system after removal of the Cp* entity in **1.** Calculation of the spin density in **C** reveals that the single electron is mainly localised in a p-like SOMO of the central P atom, but it is also partially delocalised over the tungsten carbonyl moieties. A Mullikan analysis revealed that 75% of the spin density is localised at the phosphorus atom (NBO: 56%). Visualisations of spin densities and the SOMO are shown in Figure 8.

Furthermore, the thermolysis thermodynamics of phosphinidene complex $[Cp^*P\{W(CO)_5\}_2]$ (**1**) were calculated. The corresponding calculated standard reaction enthalpies of the gas-phase reactions are listed in Table 2.

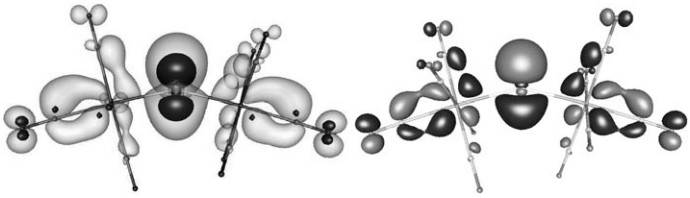

Figure 8. Isocontour surfaces of calculated spin densities (left, 0.01 and 0.001 a.u.) and of the SOMO (right, 0.05 a.u.) in **C**.

Table 2. Calculated standard reaction enthalpies of gas-phase reactions.

	Reaction	$\Delta H^0_{(298)}$ [kJ mol^{-1}]	$\Delta G^0_{(298)}$ [kJ mol^{-1}]	$\Delta G^0_{(298)}$ [kJ mol^{-1}]
I	**1**⇄$Cp^{*\bullet}$+[$^{\bullet}P\{W(CO)_5\}_2$] (**C**)	+128	+57	+36
II	**1**⇄$[Cp^*(CO)_3W{-}P{\rightarrow}W(CO)_5]$ (**A**)+2 CO	+158	+68	+42
III	**1**⇄$[Cp^*(CO)_2W{\equiv}P{\rightarrow}W(CO)_5]$ (**B**)+3 CO	+172	+24	−19
IV	**1**⇄$[(CO)_3W(\eta^5\text{-}C_5Me_4CH_2)P(H)W(CO)_5]$ (**3**)+2 CO	+81	0	−23
V	**A**⇄$[Cp^*(CO)_2W{\equiv}P{\rightarrow}W(CO)_5]$ (**B**)+CO	+14	−44	−61
VI	**A**⇄$[(CO)_3W(\eta^5\text{-}C_5Me_4CH_2)P(H)W(CO)_5]$ (**3**)	−76	−68	−66

Calculated reactions I–III are endothermic but their standard entropies are positive. Thus, one can suggest that at higher temperatures the equilibria will be shifted in favour of the final products. Subsequently, reaction III leading to the triply bonded intermediate **B** is endergonic at room temperature but exoergonic under the conditions of the thermolysis reactions in boiling toluene. Furthermore, as the standard reaction enthalpies for reactions V and VI show, if double CO loss occurs for **1**, the resulting intermediate **A** is easily transformed into intermediate **B** and the phosphine **3**. Moreover, in light of the ΔH^0 values, elimination of Cp* as a radical (reaction I) is not as high in energy as the Cp* migration processes in reactions II and III, which corresponds to its preferred occurrence in photolytic processes at ambient temperature.

To study the Cp* migration process of phosphinidene complex **1** to yield triply bonded intermediate **B**, the energetic-minima structures along the reaction coordinate were calculated by DFT methods (Figure 9). In **1**, the Cp* moiety is already oriented towards one $W(CO)_5$ group, which facilitates the first CO elimination. On removal of the second CO ligand, the Cp* moiety becomes involved in an additional η^2 bonding mode at the W atom, but remains bound to P in a η^1 mode. After displacement from the phosphorus atom, the η^2 coordination mode at the W atom changes more to η^5 coordination in intermediate **A**.[27] After the

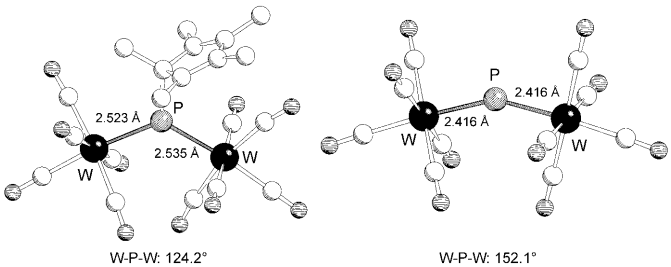

Figure 7. Calculated structures of **1** (left) and intermediate **C** (right) at the BP86/SV(P) level of theory.

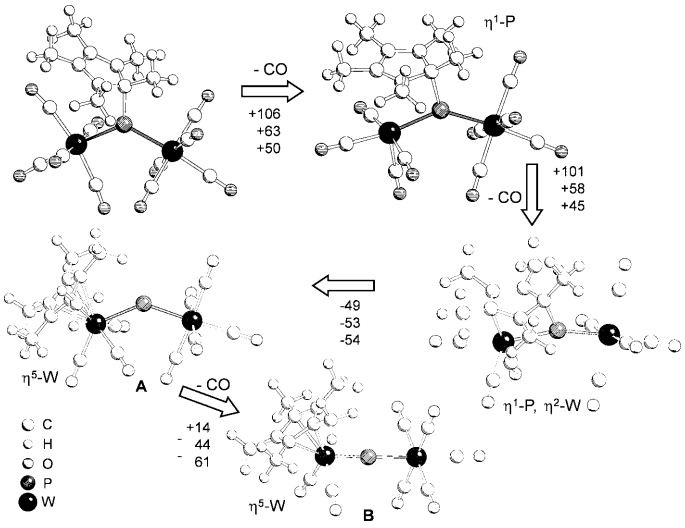

Figure 9. Calculated minima structures of the Cp* migration process of the phosphinidene complex **1** to give intermediate **B** (BP86/SV(P) level of theory). Energies [kJ mol^{-1}] at the arrows: top ΔH^0 (298.15 K), middle ΔG^0 (298.15 K) and bottom ΔG^0 (384 K).

third CO molecule is eliminated, formation of triply bonded intermediate **B** is obvious, but so is generation of complex **3** with activated C–H bond.

Reaction pathway: The proposed pathway of thermal reaction (1) shown in Scheme 3 is based on the nature of the isolated products. Formation of the main products **8** and **9** from the thermolysis of $[Cp^*P\{W(CO)_5\}_2]$ in the presence of $[\{CpMo(CO)_2\}_2]$ confirms the existence of triply bonded intermediate **B**, and they can be formally regarded as the products of a [2+2] cycloaddition reaction[28] of **B** with $[\{CpMo(CO)_2\}_2]$, in which after subsequent P–Mo and Mo–bond formation the phosphido-capped trinuclear clusters are formed. Formation of **8** with coordinated $\{W(CO)_5\}$ group and **9** without a $\{W(CO)_5\}$ moiety seems to be equally favoured (each in about 30% yield) and may be influenced by the specific steric requirements of the bulky Cp* ligand. Formation of **7** as a minor product demonstrates the existence of a second intermediate **C**, generated by elimination of the Cp* ligand. Thus, **7** can be regarded as product of the

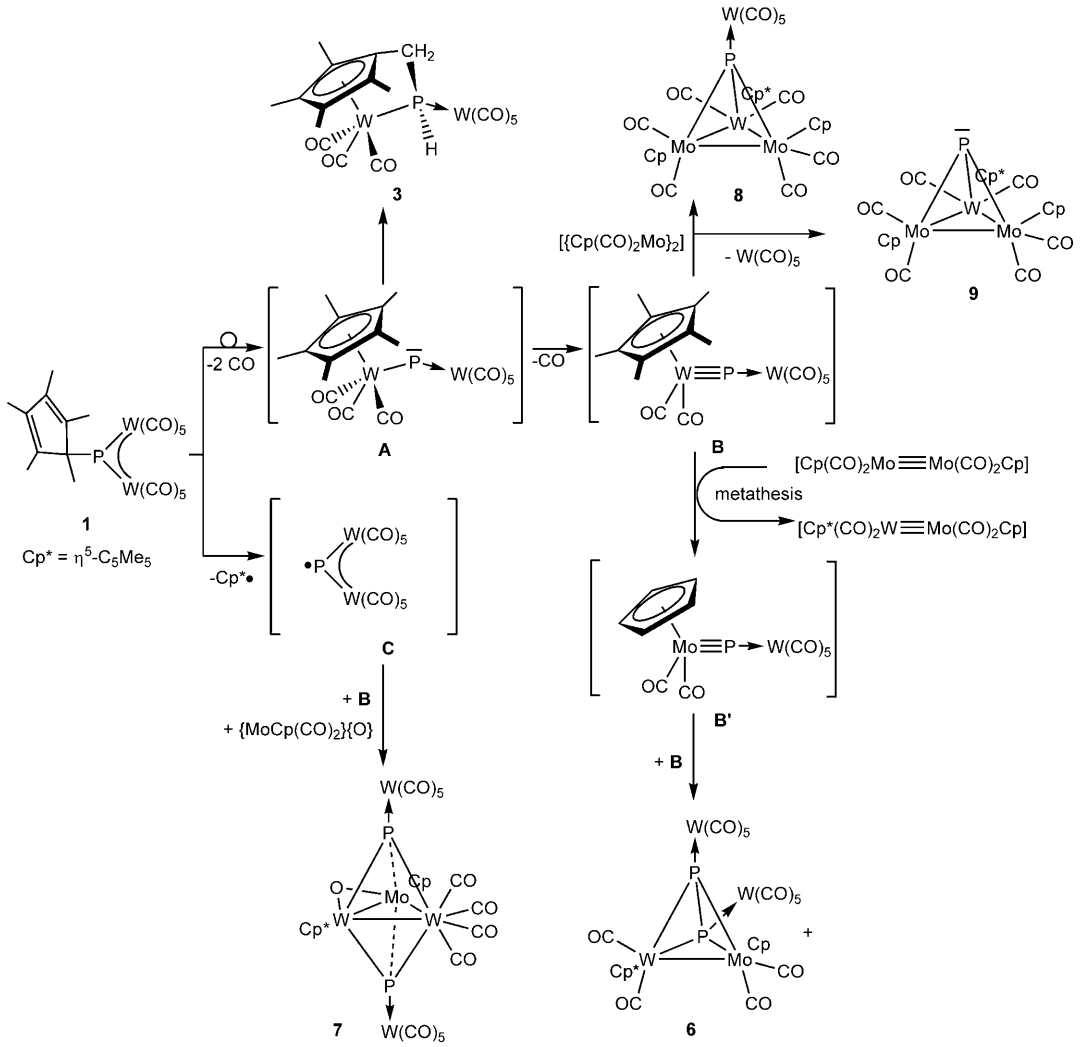

Scheme 3. Proposed reaction pathway of the thermolysis of **1** with $[\{CpMo(CO)_2\}_2]$.

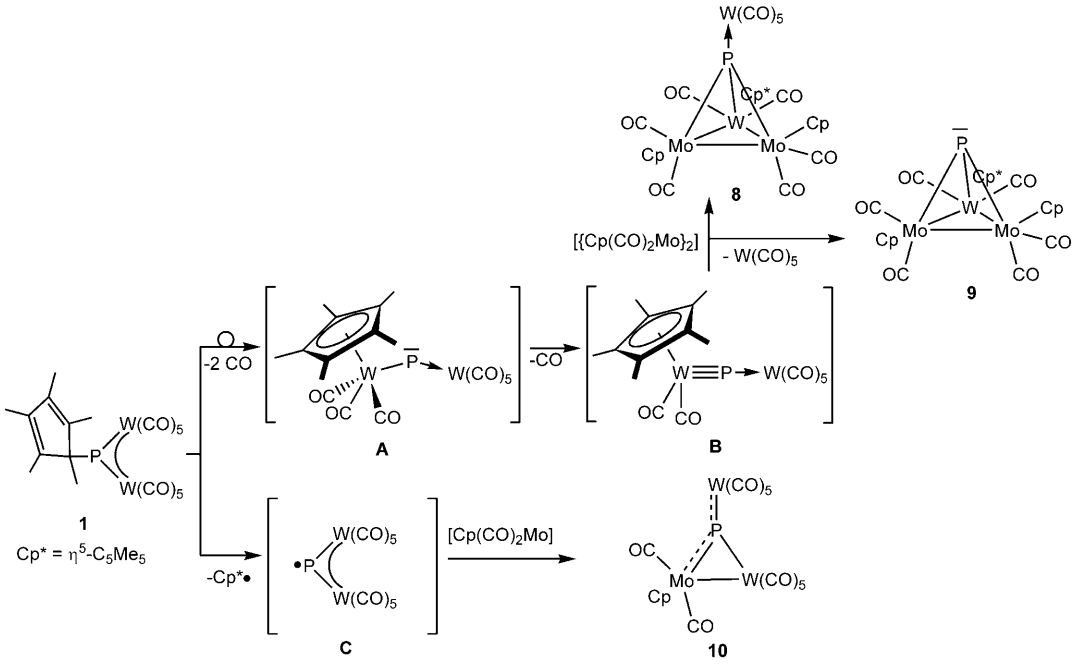

Scheme 4. Proposed reaction pathway of the photolysis of **1** with $[\{CpMo(CO)_2\}_2]$.

reaction between triply bonded intermediate **B**, intermediate **C** and a $[CpMo(CO)_2(O)]$ unit.[13] Furthermore, the appearance of **6** in about 10% yield, which contains one $\{CpMo(CO)_2\}$ unit and a $\{Cp^*W(CO)_2\}$ moiety in a tetrahedral complex, hints that during thermolysis an additional metathesis reaction occurs between intermediate **B** and the Mo dimer to give a triply bonded intermediate of formula $[Cp(CO)_2Mo{\equiv}P{\rightarrow}W(CO)_5]$ (**B′**). Intermediate **B′** undergoes dimerisation with **B** to form **6**. Tetrahedral M_2P_2 complex **6** has two $\{W(CO)_5\}$ groups, whereas the presence of only one $\{W(CO)_5\}$ moiety on the M_2P_2 tetrahedron $[Cp^*_2(CO)_4W_2(\mu,\eta^2\text{-}P_2)\{W(CO)_5\}]$ (**2**) reflects the steric influence of two Cp* groups in **2** in contrast to one Cp* and one Cp ligand in **6**.

The proposed reaction pathway of photolysis reaction (2) of $[Cp^*P\{W(CO)_5\}_2]$ in the presence of $[\{CpMo(CO)_2\}_2]$ is shown in Scheme 4 and is based on the structures of the isolated products. Formation of **9** as the main product and **8** confirm the existence of triply bonded intermediate **B**, which undergoes cyclisation reactions and subsequent metal–phosphorus and metal–metal bond formation. Since **9** is isolated in high yields and **8** is only a minor product, removal of terminal $W(CO)_5$ units seems to be more favoured under photolysis conditions in comparison to thermolysis reaction (1). Furthermore, phosphinidene complex **10** can be regarded as a reaction product of **C** and a $\{Mo(CO)_2Cp\}$ unit. Alternatively, intermediate **B′**, formed by metathesis, could react with a $\{W(CO)_5\}$ moiety to give **10**. However, the latter possible reaction should then also occur in thermolysis reaction (1), in which complex **10** could never be identified.

Conclusion

Trapping reactions of triply bonded intermediate $[Cp^*(CO)_2W{\equiv}P{\rightarrow}W(CO)_5]$ (**B**), generated by thermolysis and photolysis of $[Cp^*P\{W(CO)_5\}_2]$ (**1**), with transition-metal complexes containing multiple bonds open up broad perspectives for the synthesis of novel main group/transition metal cage compounds. By using $[Cp(CO)_2Mo{\equiv}Mo(CO)_2Cp]$ as trapping reagent, a number of new heteronuclear clusters could be synthesised in good yields and comprehensively characterised. Furthermore, the results show that the existence of intermediate **C** and the subsequent trapping reactions with reactive species are more important in photolysis than in thermolysis of **1**. Moreover, DFT calculations gave insight into the stepwise process of Cp* migration in **1** resulting in the triply bonded intermediate **B**, and also into the electronic structure of **C**. Additionally, the calculated thermodynamic data for formation of the different intermediates agree well with their experimentally observed formation conditions.

Experimental Section

General remarks: All manipulations were performed under an atmosphere of dry nitrogen by using standard Schlenk techniques. All solvents were dried by common methods and freshly distilled prior to use. NMR spectra were recorded on a Bruker AC 250 (^{1}H: 250.13 MHz; ^{31}P: 101.256 MHz; standards: ^{1}H: Me_4Si, ^{31}P: 85% H_3PO_4). IR spectra were recorded on a Bruker IFS 28 spectrometer. Mass spectra were obtained on a Varian MAT 711 (70 eV).

Reagents: The starting materials $[Cp^*P\{W(CO)_5\}_2]$[8,9] and $[\{CpMo(CO)_2\}_2]$[29] were prepared according to literature methods.

Thermolysis of [Cp*P{W(CO)$_5$}$_2$] in the presence of [{CpMo(CO)$_2$}$_2$]: synthesis of 5–9: A solution of **1** (407 mg, 0.5 mmol) and [{CpMo(CO)$_2$}$_2$] (260 mg, 0.6 mmol) in toluene (30 mL) was heated to reflux for 2 h. The solvent was removed to dryness. The dark brown residue was transferred onto silica gel and separated by column chromatography (30×2.5 cm; Macherey-Nagel, 230–400 mesh). Elution with *n*-hexane/toluene (10/3) gave a red fraction containing [{CpMo(CO)$_3$}$_2$] (**5**; 49 mg). This was followed by an orange fraction (*n*-hexane/toluene 1/1) that yielded 65 mg (10%) of **6** after recrystallisation. A yellow-green fraction was obtained from hexane/toluene (5/6); after recrystallisation from C_6D_6 **7** (75 mg, 10%) was isolated. Elution with *n*-hexane/toluene (5/9) gave an emerald fraction containing **8**, which was recrystallised from toluene to give 185 mg (30%). This was followed by a brown fraction of **9** (*n*-hexane/toluene 1:2) that yielded 126 mg (30%) after recrystallisation from toluene.

Photolysis of [Cp*P{W(CO)$_5$}$_2$] in the presence of [{CpMo(CO)$_2$}$_2$]: synthesis of 5, 8, 9 and 10: [{CpMo(CO)$_2$}$_2$] (151 mg, 0.35 mmol) was added to a solution of [Cp*P{W(CO)$_5$}$_2$] (**1**) (244 mg, 0.3 mmol) in toluene (50 mL) in a quartz glass vessel. The solution was irradiated for 2 h by UV light and the solvent was completely removed in vacuum. The resulting brown residue was transferred to silica gel and separated by column chromatography (30×2.5 cm; Macherey-Nagel, 230–400 mesh). A red fraction of [{CpMo(CO)$_3$}$_2$] (**5**) was eluted with *n*-hexane/toluene (10/3). This was followed by a green fraction of **8** (*n*-hexane/toluene 5/8) that yielded green crystals of **8** (35 mg, 10%) after recrystallisation. With *n*-hexane/toluene (1/2) a brown fraction of **9** was obtained (176 mg, 60%). A second brown fraction (*n*-hexane/toluene 1/3) afforded brown crystals of [(μ_3-PW(CO)$_5$){CpMo(CO)$_2$W(CO)$_5$}] (**10**) in 30% yield (94 mg).

Alternatively, TLC workup (silica gel on Al, Merck) under inert conditions in a glove box can be applied.

6: ^{31}P{^{1}H} NMR (121.49 MHz, C_6D_6, 25 °C): δ = −188.1 (d, ^1J(P,P) = 412.6 Hz), −301.2 ppm (d, ^1J(P,P) = 412.6 Hz); ^{1}H NMR (250.13 MHz, CD_2Cl_2, 25 °C): δ = 2.0 (s, 15H; Cp* methyl), 5.2 ppm (s, 5H; Cp); IR (KBr): $\tilde{\nu}$ = 2092 (w), 2066 (m), 2024 (w), 2001 (m, br), 1947 (s, br), 1929 (all ν(CO)) cm^{-1} (s, br); EIMS (70 eV, 200 °C): *m/z* (%): 1301 (1) [M^+], 977.7 (1.1) [M^+−W(CO)$_5$], 921.7 (1) [M^+−W(CO)$_5$−2CO], 839.7 (1.1) [M^+−W(CO)$_5$−3CO)], 653.9 (5.4) [M^+−2W(CO)$_5$], 625.9 (1.4) [M^+−2W(CO)$_5$−CO], 597.8 (6.6) [M^+−2W(CO)$_5$−2CO], 569.8 (7.8) [M^+−2W(CO)$_5$−3 (CO)], 541.8 (8.2) [M^+−2W(CO)$_5$−4CO], 406.0 (12.4) [(WMoP$_2$Cp)$^+$], 341.0 (34.16) [(WMoP$_2$)$^+$].

7: ^{31}P{^{1}H} NMR (121.49 MHz, C_6D_6, 25 °C): δ = 279.3 ppm (s, ^1J(W,P) = 200, 100, 39 Hz); ^{1}H NMR (250.13 MHz, C_6D_6, 25 °C): δ = 1.80 (s, 15H; Cp* methyl), 4.90 ppm (s, 5H; Cp); IR (KBr): $\tilde{\nu}$ = 2066 (w), 2024 (w), 1998 (m), 1971 (w), 1931 (s), 1909 (all ν(CO)) cm^{-1} (m); EIMS (70 eV, 200 °C): *m/z* (%): 1178 (0.2) [M^+−W(CO)$_5$], 977 (2.5) [M^+−W(CO)$_5$−Cp−Cp*], 949 (0.6) [M^+−W(CO)$_5$−Cp−Cp*−CO], 921 (2) [M^+−W(CO)$_5$−Cp−Cp*−2CO], 837 (1) [M^+−W(CO)$_5$−Cp−Cp*−5CO], 809 (4) [M^+−W(CO)$_5$−Cp−Cp*−6CO], 781 (1) [M^+−W(CO)$_5$−Cp−Cp*−7CO], 753 (1) [M^+−W(CO)$_5$−Cp−Cp*−8CO], 725 (3) [M^+−W(CO)$_5$−Cp−Cp*−9CO].

8: ^{31}P{^{1}H} NMR (121.49 MHz, CD_2Cl_2, 25 °C): δ = 153.8 ppm (s, ^1J(W,P) = 196, 76 Hz); ^{1}H NMR (300.13 MHz, [D$_8$]toluene, 25 °C): δ = 1.70 (s, 15H; Cp* methyl), 4.75 (s, 10H; 2Cp); IR (KBr): $\tilde{\nu}$ = 2058 (m), 1977 (m), 1942 (s), 1899 (s), 1869 (s), 1826 (all ν(CO)) cm^{-1} (m); EIMS (70 eV, 200 °C): *m/z* (%): 1098.6 (0.3) [M^+−Cp], 1033.6 (1.0) [M^+−2Cp], 839.8 (2.4) [M^+−W(CO)$_5$], 783.8 (1.9) [M^+−W(CO)$_5$−CO], 755.9 (4.1) [M^+−W(CO)$_5$−3CO], 727.9 (6.0) [M^+−W(CO)$_5$−4CO], 699.9 (15.2) [M^+−W(CO)$_5$−5CO], 671.8 (15.2) [M^+−W(CO)$_5$−6CO], 662.8 (8.6) [M^+−W(CO)$_5$−4CO−Cp], 635.7(3.0) [M^+−W(CO)$_5$−5CO−Cp], 606.8 (2.0) [M^+−W(CO)$_5$−6CO−Cp], 322.9 (1) [W(CO)$_5^+$].

9: ^{31}P{^{1}H} NMR (121.49 MHz, C_6D_6, 25 °C): δ = 500.3 ppm (s, ^1J(WP) = 40.7 Hz); ^{1}H NMR (250.13 MHz, C_6D_6, 25 °C): δ = 1.82 (s, 15H; Cp* methyl), 4.85 (s, 10H; 2Cp*); IR (KBr): $\tilde{\nu}$ = 1967 (m), 1937 (sh), 1925 (s, br), 1894 (s), 1866 (s), 1850 (m), 1777 (all ν(CO)) cm^{-1} (m); EIMS (70 eV, 200 °C): *m/z* (%): 839.8 (29) [M^+], 783.8 (13) [M^+−2CO], 755.9 (23) [M^+−3CO], 726 (43) [M^+−4CO], 700 (76) [M^+−5CO], 671.8 (77) [M^+−6CO].

10: ^{1}H NMR (250.13 MHz, [D$_8$]toluene, 25 °C): δ = 4.57 ppm (s, 5H; Cp); ^{31}P{^{1}H} NMR (121.49 MHz, [D$_8$]toluene, 25 °C): δ = 882.5 ppm (s; ^1J(W,P) = 55, 191 Hz); IR (KBr): $\tilde{\nu}$ = 2088 (w), 2062 (w, br), 2057 (w, br), 2010 (w), 1990 (w), 1954 (s, br), 1939 (m), 1922 (all ν(CO)) (m) cm^{-1}; EIMS (70 eV, 200 °C): *m/z* (%): 896 (56) [M^+], 868 (27) [M^+−CO], 840 (37) [M^+−2CO], 812 (11) [M^+−3CO], 784 (28) [M^+−4CO], 756 (28) [M^+−5CO], 728 (70) [M^+−6CO], 700 (85) [M^+−7CO], 672 (44) [M^+−8CO], 644 (34) [M^+−9CO], 616 (31) [M^+−10CO], 588 (43) [M^+−11CO], 560.8 (62) [M^+−12CO].

Crystal structure analysis: Crystal structure analyses of **6–10** were performed on a STOE IPDS diffractometer with $Mo_{K\alpha}$ radiation (λ = 0.71073 Å) for **8** and **9**, and $Ag_{K\alpha}$ radiation (λ = 0.56087 Å) for **6**, **7** and **10**. Machine parameters, crystal data, and data collection parameters are summarised in Table 1. The structures were solved by direct methods with the program SHELXS-93,[30] and full-matrix least-squares refinement on F^2 in SHELXL-97[31] was performed with anisotropic displacements for non-H atoms. Hydrogen atoms were located in idealised positions and refined isotropically according to the riding model. Complex **9** crystallises in the acentric space group $Pca2_1$ in an enantiomerically impure form [Flack parameter = 0.20(2)], and thus a TWIN refinement was applied.

CCDC 678526 (**6**), 68527 (**7**), 678523 (**8**), 678524 (**9**) and 678525 (**10**) contain the supplementary crystallographic data for this paper. These data can be obtained free of charge from The Cambridge Crystallographic Data Centre via www.ccdc.cam.ac.uk/data_request/cif.

Theoretical calculations: The quantum chemical calculations were performed at the (RI-)[32] BP86[33]/SV(P)[34] level by using the TURBOMOLE program package.[35] For the Cp* and [P{W(CO)$_5$}$_2$] radicals, the unrestricted Kohn–Sham formalism was used, and for all others the restricted Kohn–Sham formalism. Vibrational frequencies were calculated analytically with the AOFORCE[36] module. The absence of imaginary frequencies proved that all optimised structures were true minima. Thermodynamic functions were calculated with the FREEH tool included in the TURBOMOLE package. For details, see the Supporting Information.

Acknowledgements

The authors thank the Deutsche Forschungsgemeinschaft and the Fonds der Chemischen Industrie for comprehensive financial support. E.L. is grateful to the Fonds der Chemischen Industrie for a PhD fellowship, and S.Z. thanks the Alexander von Humboldt Foundation for a post-doctoral fellowship.

[1] Recent reviews for Group 15 elements: a) B. P. Johnson, G. Balázs, M. Scheer, *Top. Curr. Chem.* **2004**, *232*, 1–23; b) B. P. Johnson, G. Balázs, M. Scheer, *Coord. Chem. Rev.* **2006**, *250*, 1178–1195; for Group 15 and Group 14 elements: c) G. Balázs, L. Gregoriades, M. Scheer, *Organometallics* **2007**, *26*, 3058–3075; for Group 14 elements: d) M. Weidenbruch, *Angew. Chem.* **2003**, *115*, 2322–2324; *Angew. Chem. Int. Ed.* **2003**, *42*, 2222–2224.

[2] a) C. E. Laplaza, W. M. Davis, C. C. Cummins, *Angew. Chem.* **1995**, *107*, 2181–2183; *Angew. Chem. Int. Ed. Engl.* **1995**, *34*, 2042–2044; b) J. S. Figueroa, C. C. Cummins, *J. Am. Chem. Soc.* **2004**, *126*, 13916–13917.

[3] a) N. C. Zanetti, R. R. Schrock, W. M. Davis, *Angew. Chem.* **1995**, *107*, 2184–2186; *Angew. Chem. Int. Ed. Engl.* **1995**, *34*, 2044–2046; b) N. C. Mösch-Zanetti, R. R. Schrock, W. M. Davis, K. Wanninger, S. W. Seidel, M. B. O'Donoghue, *J. Am. Chem. Soc.* **1997**, *119*, 11037.

[4] a) M. Scheer, J. Müller, M. Häser, *Angew. Chem.* **1996**, *108*, 2637–2641; *Angew. Chem. Int. Ed. Engl.* **1996**, *35*, 2492–2496; b) G. Balázs, M. Sierka, M. Scheer, *Angew. Chem.* **2005**, *117*, 4999–5003; *Angew. Chem. Int. Ed.* **2005**, *44*, 4920–4924; c) G. Balázs, J. C. Green, M. Scheer, *Chem. Eur. J.* **2006**, *12*, 8603–8608.

[5] a) P. Kramkowski, G. Baum, U. Radius, M. Kaupp, M. Scheer, *Chem. Eur. J.* **1999**, *5*, 2890–2898; b) M. Scheer, P. Kramkowski, K. Schuster, *Organometallics* **1999**, *18*, 2874–2883.

[6] M. Scheer, *Coord. Chem. Rev.* **1997**, *163*, 271–286; see also ref. [1c].
[7] a) M. E. Garcia, V. Riera, M. A. Ruiz, D. Saez, H. Hamidov, J. C. Jeffery, T. Riis-Johannessen, *J. Am. Chem. Soc.* **2003**, *125*, 13044–13045; b) I. Amor, M. Garcia, M. A. Ruiz, D. Saez, H. Hamidov, J. C. Jeffery, *Organometallics* **2006**, *25*, 4857–4869.
[8] a) R. Kroos, PhD thesis, Universität Bielefeld, **1989**; b) P. Jutzi, R. Kroos, *J. Organomet. Chem.* **1990**, *390*, 317–322.
[9] M. Scheer, E. Leiner, P. Kramkowski, M. Schiffer G. Baum, *Chem. Eur. J.* **1998**, *4*, 1917–1923.
[10] M. Schiffer, E. Leiner, M. Scheer, *Eur. J. Inorg. Chem.* **2001**, 1661–1663.
[11] M. Schiffer, M. Scheer, *Chem. Eur. J.* **2001**, *7*, 1855–1861.
[12] M. Scheer, D. Himmel, B. P. Johnson, C. Kuntz, M. Schiffer, *Angew. Chem.* **2007**, *119*, 4045–4049; *Angew. Chem. Int. Ed.* **2007**, *46*, 3971–3975.
[13] It seems that the origin of **7** is dependent on traces of oxygen in the synthesis of triply bonded Mo starting material $[\{CpMo(CO)_2\}_2]$, since different charges of $[\{CpMo(CO)_2\}_2]$ gave slightly different quantities of **7** in reaction (1).
[14] G. Huttner, K. Evertz, *Acc. Chem. Res.* **1986**, *19*, 406–413, and references therein.
[15] G. Huttner, U. Weber, B. Sigwarth, O. Scheisteger, H. Lang, L. Zsolnai, *J. Organomet. Chem.* **1985**, *282*, 331–348.
[16] A. Simon, H. Borrmann, J. Horakh, *Chem. Ber.* **1997**, *130*, 1235–1240.
[17] G. A. Carriedo, J. A. K. Howard, J. C. Jeffery, K. Sneller, F. G. A. Stone, A. M. M Weerasuria, *J. Chem. Soc. Dalton Trans.* **1990**, 953–958.
[18] A. Patel, S. Siddiqui, D. T. Richens, M. E. Harman, M. B. Hursthouse, *J. Chem. Soc. Dalton Trans.* **1993**, 767–774.
[19] S.-G. Shyu, J.-Y. Hsu, P.-J. Lin, W.-J. Wu, S.-M. Peng, G.-H. Lee, Y.-S. Wen, *Organometallics* **1994**, *13*, 1699–1710.
[20] J. E. Davies, M. J. Mays, E. J. Pook, P. R. Reithby, P. K. Tompkin, *Chem. Commun.* **1997**, 1997–1998.
[21] M. J. Aroney, I. E. Buys, M. S. Davies, T. W. Hambley, *J. Chem. Soc. Dalton Trans.* **1994**, 2827–2834.
[22] J. E. Davies, M. C. Klunduk, M. J. Mays, P. R. Raithby, G. P. Shields, P. K. Tompkin, *J. Chem. Soc. Dalton Trans.* **1997**, 715–719.
[23] G. Huttner, U. Weber, B. Sigwarth, O. Scheidsteger, H. Lang, Z. Laszlo, *J. Organomet. Chem.* **1985**, *282*, 331–348.
[24] K. V. Adams, N. Choi, G. Conole, J. E. Davies, J. D. King, M. J. Mays, M. McPartlin, P. R. Raithby, *J. Chem. Soc. Dalton Trans.* **1999**, 3679–3686.
[25] M. Scheer, J. Müller, G. Baum, M. Häser, *Chem. Commun.* **1998**, 1051–1052.
[26] K. Lammertsma, *Top. Curr. Chem.* **2003**, *229*, 95–119.
[27] Intermediate **A** has three sets of slightly different W–C distances (2×2.398, 2×2.477, 1×2.573 Å).
[28] For carbon systems a concerted reaction along the idealised C_s reaction coordinate with orthogonal approach of two triple bonds is an orbitally forbidden process. However, for such processes in which transition metals are involved, a suprafacial [2+2] addition is calculated to be of lower energy: T. Woo, E. Folga, T. Ziegler, *Organometallics* **1993**, *12*, 1289–1298.
[29] Herrmann Brauer, *Synthetic Methods of Organometallic and Inorganic Chemistry, Vol. 8, Transition Metal Chemistry Part 2*, Georg Thieme, Stuttgart **1997**, p. 60.
[30] G. M. Sheldrick, SHELXS-93, University of Göttingen, **1993**.
[31] G. M. Sheldrick, SHELXL-97, University of Göttingen, **1997**.
[32] K. Eichkorn, O. Treutler, H. Oehm, M. Häser, R. Ahlrichs, *Chem. Phys. Lett.* **1995**, *242*, 652–660.
[33] a) A. D. Becke, *Phys. Rev. A* **1988**, *38*, 3098–3100; b) J. P. Perdew, *Phys. Rev. B* **1986**, *33*, 8822–8824; erratum: J. P. Perdew, *Phys. Rev. B* **1986**, *34*, 7406.
[34] A. Schäfer, H. Horn, R. Ahlrichs, *J. Chem. Phys.* **1992**, *97*, 2571.
[35] a) R. Ahlrichs, M. Bär, M. Häser, H. Horn, C. Kölmel, *Chem. Phys. Lett.* **1989**, *162*, 165–169; b) O. Treutler, R. Ahlrichs, *J. Chem. Phys.* **1995**, *102*, 346–354.
[36] a) P. Deglmann, F. Furche, R. Ahlrichs, *Chem. Phys. Lett.* **2002**, *362*, 511; b) P. Deglmann, F. Furche, *J. Chem. Phys.* **2002**, *117*, 9535.

Received: April 28, 2008
Published online: August 11, 2008

